Article

Self-Assembled Monolayers Derived from a Double-Chained Monothiol Having Chemically Dissimilar Chains

Shishan Zhang, Andrew C. Jamison, Daniel K. Schwartz, and T. Randall Lee

Langmuir, **2008**, 24 (18), 10204-10208• DOI: 10.1021/la801397t • Publication Date (Web): 13 August 2008

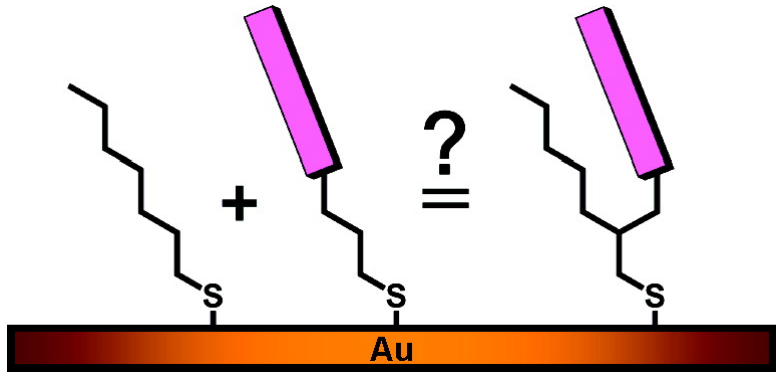

More About This Article

Additional resources and features associated with this article are available within the HTML version:

- Supporting Information
- Links to the 1 articles that cite this article, as of the time of this article download
- Access to high resolution figures
- Links to articles and content related to this article
- Copyright permission to reproduce figures and/or text from this article

View the Full Text HTML

Self-Assembled Monolayers Derived from a Double-Chained Monothiol Having Chemically Dissimilar Chains

Shishan Zhang,[†] Andrew C. Jamison,[†] Daniel K. Schwartz,[‡] and T. Randall Lee*,[†]

Departments of Chemistry and Chemical Engineering, University of Houston, Houston, Texas 77204-5003, and Department of Chemical and Biological Engineering, University of Colorado, Boulder, Colorado 80309-0424

Received May 5, 2008. Revised Manuscript Received June 11, 2008

The structure and conformation of self-assembled monolayers (SAMs) derived from the adsorption of a specifically designed double-chained partially fluorinated thiol having the formula 12,12,13,13,14,14,15,15,16,16,17,17,18,18,19,19,19-heptadecafluoro-2-tetradecylnona-decane-1-thiol (**2**) onto the surface of evaporated gold were examined by ellipsometry, contact angle goniometry, polarization modulation infrared reflection−absorption spectroscopy (PM-IRRAS), and X-ray photoelectron spectroscopy (XPS). The results were compared to those of SAMs generated from normal hexadecanethiol (**1**) and a structurally related single-chained partially fluorinated thiol having the formula 12,12,13,13,14,14,15,15,16,16,17,17,18,18,19,19,19-heptadecafluorononadecane-1-thiol (**3**). Collectively, the studies demonstrate that the double-chained adsorbate **2** forms SAMs on gold in which the alkyl chains are less densely packed and less conformationally ordered than those in the SAMs derived from each of the single-chained adsorbates. Furthermore, the fluorocarbon moieties in the SAMs derived from **2** are more tilted from the surface normal than those in the SAMs derived from **3**. The low values of contact angle hysteresis suggest, however, that the double-chained adsorbate **2** generates homogeneous monolayer films on the surface of gold.

Introduction

Phase separation has been frequently observed in mixed monolayer films, including Langmuir−Blodgett (LB)[1−10] and self-assembled monolayer (SAM)[11−15] systems. A number of intermolecular interactions have been shown to induce phase separation in mixed monolayer systems, including aliphatic vs aromatic hydrocarbons,[1,2,13,15−18] polycyclic vs aliphatic hydrocarbons,[19−21] saturated vs unsaturated (or branched) alkyl chains,[4,5,9,22] long vs short aliphatic chains,[1,20] hydrogenated vs fluorinated chains,[2,3,6−8,10,12,14,16−18] and even more subtle types of chemical dissimilarities for the terminal groups, such as combinations of the following groups: CO_2H,[23,24] CO_2CH_3,[25] CN,[11] OH,[26,27] and ferrocenyl.[28] Generally, these phase-separated domains have a random and broad size distribution. Many potential applications, including molecular electronics,[29] sensing via molecular recognition,[30] and replication of the functionality of biological surfaces or membranes[25] (e.g., lipid bilayers)[31] require complicated mixed-surface functionalities, where the relative proportions of functional groups as well as their aggregate size and shape must be controlled at the meso- or nanoscale.

One of the primary goals of our research is to develop mixed SAM systems that exhibit predictable and well-defined phase behavior through the utilization of equilibrium methods. The strategy is analogous to that used in the generation of bulk (three-dimensional, 3-D) micelles and microemulsions - namely, controlling the size of the phase-separated domains by adding an additional component that is line-active, that is, it partitions to the phase boundaries. For 3-D systems, depending largely on the concentrations of the components, the aggregates can be spherical, oblong, cylindrical, or planar (bilayer). In 3-D microemulsions, the presence of an appropriate surface-active

* To whom correspondence should be addressed. E-mail: trlee@uh.edu.
[†] University of Houston.
[‡] University of Colorado.

(1) Sparr, E.; Ekelund, K.; Engblom, J.; Engstroem, S.; Wennerstroem, H. *Langmuir* **1999**, *15*, 6950.
(2) Shibata, O.; Yamamoto, S. K.; Lee, S.; Sugihara, G. *J. Colloid Interface Sci.* **1996**, *184*, 201.
(3) Shibata, O.; Krafft, M. P. *Langmuir* **2000**, *16*, 10281.
(4) Solletti, J. M.; Botreau, M.; Sommer, F.; Brunat, W. L.; Kasas, S.; Duc, T. M.; Celio, M. R. *Langmuir* **1996**, *12*, 5379.
(5) Solletti, J. M.; Botreau, M.; Sommer, F.; Tran Minh, d.; Celio, M. R. *J. Vac. Sci. Technol. B* **1996**, *14*, 1492.
(6) Meyer, E.; Overney, R.; Luethi, R.; Brodbeck, D.; Howald, L.; Frommer, J.; Guentherodt, H. J.; Wolter, O.; Fujihira, M.; et al. *Thin Solid Films* **1992**, *220*, 132.
(7) Overney, R. M.; Meyer, E.; Frommer, J.; Guentherodt, H. J.; Fujihira, M.; Takano, H.; Gotoh, Y. *Langmuir* **1994**, *10*, 1281.
(8) Lehmler, H.-J.; Jay, M.; Bummer, P. M. *Langmuir* **2000**, *16*, 10161.
(9) Leporatti, S.; Bringezu, F.; Brezesinski, G.; Moehwald, H. *Langmuir* **1998**, *14*, 7503.
(10) Fujihira, M.; Takano, H. *Thin Solid Films* **1994**, *243*, 446.
(11) Stranick, S. J.; Atre, S. V.; Parikh, A. N.; Wood, M. C.; Allara, D. L.; Winograd, N.; Weiss, P. S. *Nanotechnology* **1996**, *7*, 438.
(12) Ishida, T.; Mizutani, W.; Choi, N.; Ogiso, H.; Azehara, H.; Hokari, H.; Akiba, U.; Fujihira, M.; Kojima, I.; Tokumoto, H. *Colloids Surf. A* **1999**, *154*, 219.
(13) Mathauer, K.; Frank, C. W. *Langmuir* **1993**, *9*, 3446.
(14) Ishida, T.; Mizutani, W.; Tokumoto, H.; Hokari, H.; Azehara, H.; Fujihira, M. *Appl. Surf. Sci.* **1998**, *130−132*, 786.
(15) Hayes, W. A.; Kim, H.; Yue, X.; Perry, S. S.; Shannon, C. *Langmuir* **1997**, *13*, 2511.
(16) Dupres, V.; Cantin, S.; Benhabib, F.; Perrot, F. *Europhys. Lett.* **1999**, *48*, 86.
(17) Imae, T.; Takeshita, T.; Kato, M. *Langmuir* **2000**, *16*, 612.
(18) Monobe, H.; Koike, A.; Muramatsu, H.; Chiba, N.; Yamamoto, N.; Ataka, T.; Fujihira, M. *Ultramicroscopy* **1998**, *71*, 287.
(19) Anderson, T. G.; McConnell, H. M. *J. Phys. Chem. B* **2000**, *104*, 9918.
(20) Ekelund, K.; Sparr, E.; Engblom, J.; Wennerstroem, H.; Engstroem, S. *Langmuir* **1999**, *15*, 6946.
(21) Silvius, J. R.; Giudice, D. d.; Lafleur, M. *Biochemistry* **1996**, *35*, 15198.
(22) Nag, K.; Keough, K. M. W *Biophys. J.* **1993**, *65*, 1019.
(23) Lee, T. R.; Carey, R. I.; Biebuyck, H. A.; Whitesides, G. M. *Langmuir* **1994**, *10*, 741.
(24) Kakiuchi, T.; Sato, K.; Iida, M.; Hobara, D.; Imabayashi, S.; Niki, K. *Langmuir* **2000**, *16*, 7238.
(25) Stranick, S. J.; Parikh, A. N.; Tao, Y. T.; Allara, D. L.; Weiss, P. S. *J. Phys. Chem.* **1994**, *98*, 7636.
(26) Atre, S. V.; Liedberg, B.; Allara, D. L. *Langmuir* **1995**, *11*, 3882.
(27) Brewer, N. J.; Leggett, G. J. *Langmuir* **2004**, *20*, 4109.
(28) Rowe, G. K.; Creager, S. E. *Langmuir* **1994**, *10*, 1186.
(29) Iimura, K.; Shiraku, T.; Kato, T. *Langmuir* **2002**, *18*, 10183.
(30) Yang, W. R.; Hibbert, D. B.; Zhang, R.; Willett, G. D.; Gooding, J. J. *Langmuir* **2005**, *21*, 260.
(31) Ocko, B. M.; Kelley, M. S.; Nikova, A. T.; Schwartz, D. K. *Langmuir* **2002**, *18*, 9810.

10.1021/la801397t CCC: $40.75
Published on Web 08/13/2008

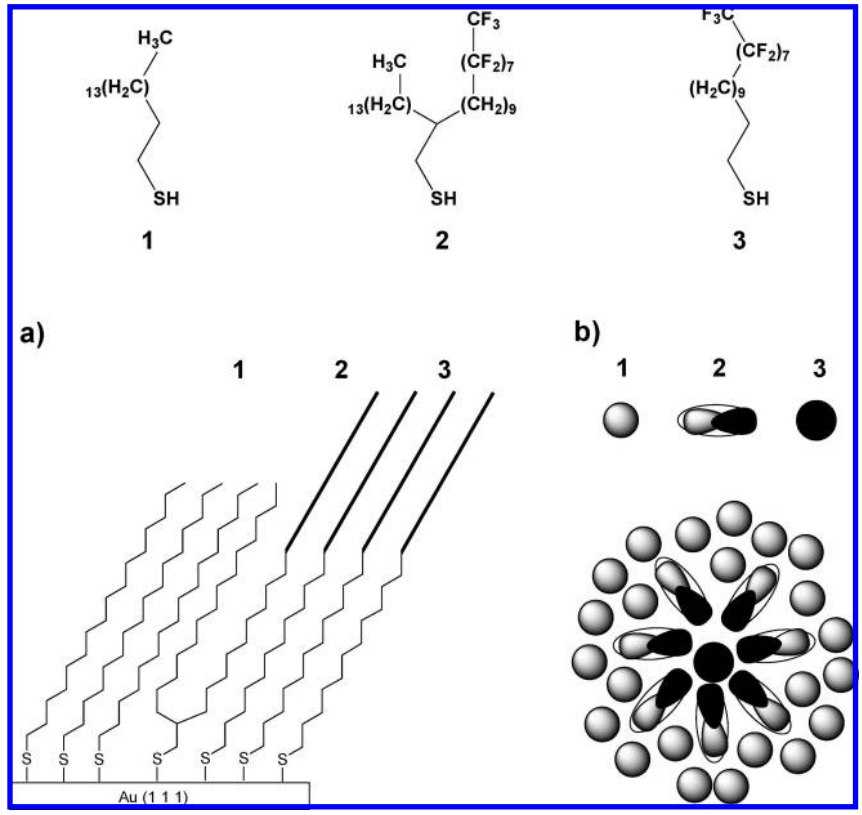

Figure 1. Structures of normal hexadecanethiol (**1**), the double-chained monothiol (**2**), and the corresponding partially fluorinated single-chained monothiol (**3**). Models of phase-separated molecular aggregates stabilized by **2**: (a) cross-section of a linactant-directed phase boundary and (b) top view of a hypothetical linactant-directed 2-D microemulsion.

component serves to reduce interfacial free energy to a sufficiently low value that macroscopic phase separation is no longer favored because the entropy of having many smaller droplets (or a convoluted bicontinuous structure) outweighs the interfacial energy cost. Thus, analogous phase behavior might be observed in a two-dimensional (2-D) regime by using specifically designed adsorbate molecules. Because such molecules are created to modify the line tension of nano- and meso-scale surface features, playing a role in monolayer phase development analogous to that of surfactants in bulk solution phases, we refer to these molecules as "linactants".[32,33] Thus, our initial thiol-based, double-chained adsorbate molecule (**2**) is designed to provide in two dimensions surfactant characteristics with respect to defining phase boundaries on a surface, as illustrated in Figure 1 (i.e., one chain prefers the aliphatic domain and the other chain prefers the fluorinated domain). In the studies under consideration, the fundamental phases will be associated with molecules **1** and **3**, while the linactant is molecule **2**. Examples of possible phase behavior are also shown in Figure 1.

As a necessary first step toward detailed studies of binary and ternary mixtures, this manuscript provides a fundamental investigation of SAMs formed from first-generation linactant **2**, designed specifically for adsorption onto gold. In **2**, we carefully chose an adsorbate architecture consisting of a single thiol headgroup (rather than a dithiol or trithiol headgroup)[34–36] to encourage surface mobility and thus to impart efficient linactant behavior. To our knowledge, there exists in the literature only a single report of SAMs on gold generated from a series of adsorbate molecules having a structure conceptually similar to that of **2**.[37] The previous study, however, focused on the packing densities and tilt angles of the single-component SAMs made from nonfluorinated, double-chained thiols. In contrast, the present study provides a detailed description of the synthesis of **2** and a thorough characterization of the SAMs formed by the adsorption of **2** onto freshly evaporated "flat" gold substrates. Analyses of the SAMs by ellipsometry, contact angle goniometry, polarization modulation infrared reflection-adsorption spectroscopy (PM-IRRAS), and X-ray photoelectron spectroscopy (XPS) are compared to those obtained from SAMs generated by the adsorption of the single-chained thiols **1** and **3**, whose structures are analogous to each of the chains comprising the tailgroup of **2**.

Experimental Section

A complete description of the materials, procedures, and instrumentation used to conduct the research reported here is provided as Supporting Information.[38,39]

Results and Discussion

Ellipsometric Thicknesses. As shown in Table 1, the ellipsometric measurements indicate thicknesses of 20, 18, and 19 Å (equal within experimental uncertainty) for the SAMs

(32) Trabelsi, S.; Zhang, S.; Lee, T. R.; Schwartz, D. K. *Soft Matter* **2007**, *3*, 1518.
(33) Trabelsi, S.; Zhang, S.; Lee, T. R.; Schwartz, D. K. *Phys. Rev. Lett.* **2008**, *100*, 037802.
(34) Shon, Y.-S.; Lee, S.; Perry, S. S.; Lee, T. R. *J. Am. Chem. Soc.* **2000**, *122*, 1278.
(35) Shon, Y.-S.; Lee, S.; Colorado, R., Jr.; Perry, S. S.; Lee, T. R. *J. Am. Chem. Soc.* **2000**, *122*, 7556.
(36) Park, J.-S.; Vo Andy, N.; Barriet, D.; Shon, Y.-S.; Lee, T. R. *Langmuir* **2005**, *21*, 2902.
(37) Chechik, V.; Schoenherr, H.; Vancso, G. J.; Stirling, C. J. M. *Langmuir* **1998**, *14*, 3003.
(38) Graupe, M.; Koini, T.; Wang, V. Y.; Nassif, G. M.; Colorado, R., Jr.; Villazana, R. J.; Dong, H.; Miura, Y. F.; Shmakova, O. E.; Lee, T. R. *J. Fluorine Chem.* **1999**, *93*, 107.
(39) Frey, S.; Heister, K.; Zharnikov, M.; Grunze, M.; Tamada, K.; Colorado, R, Jr.; Graupe, M.; Shmakova, O. E.; Lee, T. R. *Isr. J. Chem* **2000**, *40*, 81.

Table 1. Ellipsometric Thicknesses, Advancing Contact Angles, and the Calculated Hysteresis for SAMs on Gold Derived from 1, 2, and 3

adsorbate	thickness, ±2 Å	advancing contact angles, $\theta_a \pm 1°$ (hysteresis $\Delta\theta = \theta_a - \theta_r$)[a]	
		HD	water
1	20	52(6)	113(6)
2	18	73(12)	125(13)
3	19	83(11)	127(10)

[a] Receding Angles, θ_r.

derived from **1**, **2**, and **3**, respectively, assuming a constant value of 1.45 as the refractive index for all of the films. Importantly, the thicknesses of the SAMs derived from **1** and **3** are consistent with those found in literature reports of hydrocarbon[40,41] and partially fluorinated[42,43] SAMs on gold. Furthermore, while the SAMs derived from **2** might plausibly be expected to generate SAMs with relatively low values of ellipsometric thickness (due to reduced interchain packing arising from (1) its branched nature and/or (2) unfavorable hydrocarbon fluorocarbon interactions), the data fail to reflect this expectation.

Contact Angle Wettabilities. Advancing and receding contact angle measurements provide a sensitive probe of the composition, packing, and orientation of organic thin films.[35] Furthermore, the contact angle hysteresis ($\Delta\theta = \theta_a - \theta_r$) provides a measure of the degree of surface roughness or heterogeneity of the interface.[44] Using water and hexadecane as probe liquids, we measured the contact angles and the respective hystereses on SAMs derived from **1**, **2**, and **3** (see Table 1). The advancing contact angles of water and hexadecane on the SAMs derived from **1** and **3** are consistent with previously observed values,[45,46] suggesting that the quality of the gold substrates and the composition of the molecular adsorbates match our expectations. Moreover, the values of contact angle hysteresis fall within the range commonly observed for hydrocarbon[35,36] and partially fluorinated SAMs on gold,[46,47] suggesting that the films examined here possess no large-scale roughness or heterogeneity. Importantly, the contact angles of the SAM derived from **2** fall between those of the SAMs derived from **1** and **3**, which is consistent with an interface composed of a mixture of hydrocarbon and perfluorocarbon species. Similarly, the values of hysteresis for the SAM derived from **2** are comparable to those of the terminally fluorinated SAM, again suggesting a macroscopically smooth and homogeneous interface.

X-Ray Photoelectron Spectroscopy (XPS). The C_{1s}, F_{1s}, and S_{2p} XPS spectra of the SAMs derived from **1**, **2**, and **3** are shown in Figure 2. The adsorption of intact **1**, **2**, and **3** is confirmed by the C_{1s} and F_{1s} XPS spectra in Figure 2a and 2b, respectively. For XPS, the binding energy of an electron in an atom is a function of the type of atom and its environment.[48] Another factor that influences binding energy is the electrical conductivity of the sample.[48] For SAMs derived from normal alkanethiol on gold, it has been reported that the binding energy of the C_{1s} photoelectron shifts to a lower value when the alkyl chain length decreases.[49,50] The C_{1s} binding energy can therefore be used as a rough measure of the thickness and/or coverage of SAMs. Figure 2a shows a small but reproducible shift of the C_{1s} CH_2 peak to lower binding energy for the SAMs derived from **2** (−0.7 eV) and **3** (−0.3 eV) when compared to the densely packed SAMs derived from **1**. From the observed shifts, the relative

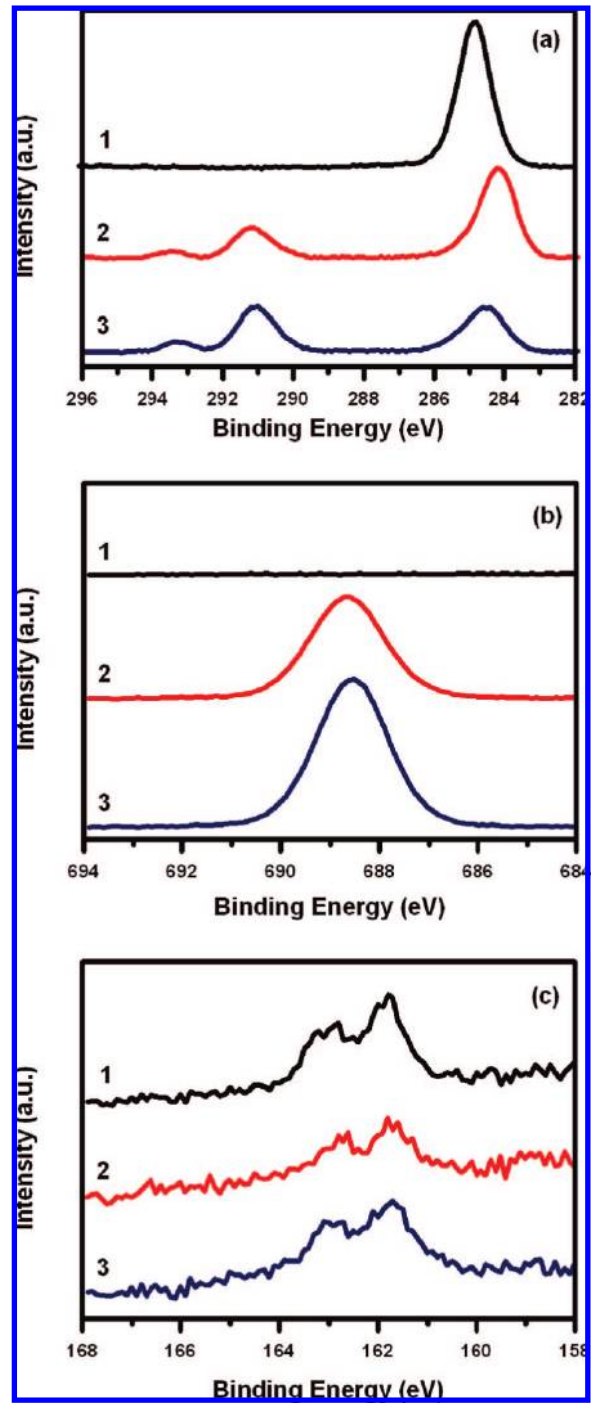

Figure 2. XPS spectra of SAMs generated by the adsorption of **1**, **2**, and **3** onto evaporated gold substrates: (a) C_{1s} region, (b) F_{1s} region, and (c) S_{2p} region.

(40) Porter, M. D.; Bright, T. B.; Allara, D. L.; Chidsey, C. E. D. *J. Am. Chem. Soc.* **1987**, *109*, 3559.
(41) Shon, Y.-S.; Lee, T. R. *Langmuir* **1999**, *15*, 1136.
(42) Colorado, R., Jr.; Graupe, M.; Shmakova, O. E.; Villazana, R. J.; Lee, T. R. *ACS Symp. Ser.* **2001**, *781*, 276.
(43) Tamada, K.; Ishida, T.; Knoll, W.; Fukushima, H.; Colorado, R., Jr.; Graupe, M.; Shmakova, O. E.; Lee, T. R. *Langmuir* **2001**, *17*, 1913.
(44) Ulman, A. *Chem. Rev.* **1996**, *96*, 1533.
(45) Tamada, K.; Nagasawa, J.; Nakanishi, F.; Abe, K.; Hara, M.; Knoll, W.; Ishida, T.; Fukushima, H.; Miyashita, S.; Usui, T.; Koini, T.; Lee, T. R. *Thin Solid Films* **1998**, *327−329*, 150.
(46) Colorado, R., Jr.; Lee, T. R. *Langmuir* **2003**, *19*, 3288.
(47) Fukushima, H.; Seki, S.; Nishikawa, T.; Takiguchi, H.; Tamada, K.; Abe, K.; Colorado, R.; Graupe, M.; Shmakova, O. E.; Lee, T. R. *J. Phys. Chem. B* **2000**, *104*, 7417.
(48) *Surface Analysis: The Principal Techniques*; Vickerman, J. C., Ed. ; Wiley: Chichester, 1997.
(49) Bain, C. D.; Troughton, E. B.; Tao, Y.-T.; Evall, J.; Whitesides, G. M.; Nuzzo, R. G. *J. Am. Chem. Soc.* **1989**, *111*, 321.
(50) Biebuyck, H. A.; Bain, C. D.; Whitesides, G. M. *Langmuir* **1994**, *10*, 1825.

packing density and/or film thickness of the SAMs can be estimated to be **1** > **3** > **2**, which is consistent with the aforementioned ellipsometric thickness measurements (vide supra). We note, however, that the C_{1s} binding energy can be influenced by other factors, including the orientation of the alkyl chains. For the SAMs derived from **2**, the peak corresponding to the CH_2 groups is distinctly unsymmetrical. The lack of symmetry might arise from the splitting of the C_{1s} CH_2 peak associated with the different chemical environments of the CH_2 entities in the two carbon chains of the double-chained thiol.

In the C_{1s} spectra of the SAMs derived from **2** and **3** (Figure 2a), the peaks related to the CF_3 (293.3 eV) and CF_2 moieties (291.1 eV) can be readily distinguished from those corresponding to the CH_2 moieties (284−285 eV). The intensity of the CH_2 peak is stronger for the SAM derived from **2** than it is for the SAM derived from **3**, which is consistent with the molecular composition of the adsorbates. Similarly, the intensities of the CF_2 and CF_3 peaks for the SAM derived from **2** are weaker than those for the SAM derived from **3**, which can be directly related to the packing densities of the fluorocarbon chains in the respective SAMs. Figure 2b shows further that the relative intensities of the F_{1s} peak (686.6 eV) also reflect the relative surface coverage of the fluorocarbon chains.

The poor signal-to-noise ratio in the S_{2p} spectra (Figure 2c) is related to the attenuation of the corresponding signal by the overlayer and/or coverage of the extended chains of the SAMs. In these spectra, a single S_{2p} doublet at 162.0 eV ($S_{2p3/2}$) is observed. The binding energies of these doublets are consistent with thiolate species bonded to the surfaces of gold.[51] Thus, the S_{2p} spectra indicate the presence of only one sulfur species and suggest strong bonding of all the investigated molecules to the gold substrate via their sulfur headgroup upon adsorption. Furthermore, the notably weaker intensity of the S_{2p} doublet for the SAM derived from **2** agrees well with the lower coverage of sulfur atoms expected for this adsorbate.

Polarization Modulation Infrared Reflection Absorption Spectroscopy (PM-IRRAS). The IRRAS spectra of the SAMs on gold are depicted in Figure 3a (C−H stretching region) and 3b (C−F stretching region). The C−H stretching region is known to be highly sensitive to the conformational order of the alkyl chains and the environment of the chains.[52] In particular, the degree of conformational order of the alkyl chains can be estimated from the frequency and width of the methylene antisymmetric band ($\nu_a^{CH_2}$) and the methylene symmetric band ($\nu_s^{CH_2}$).[40,52–54] The methylene antisymmetric band ($\nu_a^{CH_2}$) of crystalline polyethylene appears at 2920 cm^{-1}, while that of liquid polyethylene appears at 2928 cm^{-1}; likewise, the methylene symmetric band ($\nu_s^{CH_2}$) of crystalline polyethylene appears at 2850 cm^{-1}, while that of liquid polyethylene appears at 2856 cm^{-1}.[40,52]

For the SAMs derived from **1**, **2**, and **3**, the spectral region of the C−H stretching modes is shown in Figure 3a. Notably, the spectrum of the SAM generated from **1** shows additional methyl symmetric and antisymmetric stretching bands at 2877 cm^{-1} and 2965 cm^{-1}, respectively, consistent with the molecular structure of **1**. The spectra of SAMs generated from both **1** and **3** exhibit indistinct methylene symmetric and antisymmetric stretching band positions at 2850 cm^{-1} and 2918 cm^{-1}, respectively. These band positions are characteristic of the trans-

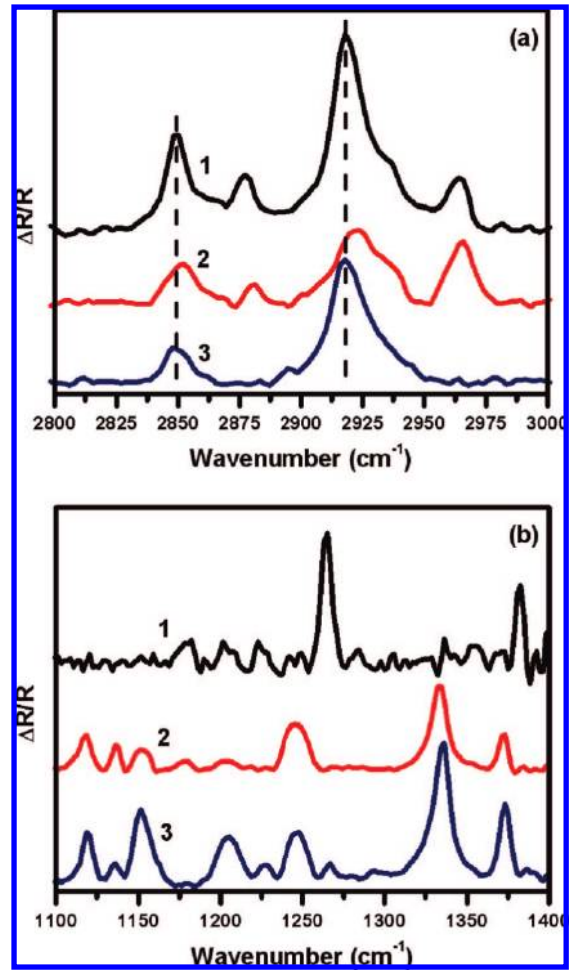

Figure 3. PM-IRRAS spectra of SAMs generated by the adsorption of **1**, **2**, and **3** onto evaporated gold substrates: (a) C−H stretching region and (b) C−F stretching region.

extended zigzag conformation of hydrocarbon chains associated with well-ordered "crystalline" SAMs (i.e., where the methylene chains in the films possess a high degree of conformational order).[52] In contrast, the spectrum of the SAM generated from **2** shows significant shifts of these bands to higher wavenumbers: $\nu_s^{CH_2}$ band at 2853 cm^{-1}, $\nu_s^{CH_3}$ band at 2880 cm^{-1}, $\nu_a^{CH_2}$ band at 2923 cm^{-1} and $\nu_a^{CH_3}$ band at 2966 cm^{-1}. The increase in wavenumber suggests that the methylene chains in the SAM derived from **2** are less conformationally ordered (or less crystalline) than those in the SAMs derived from **1** or **3**, which can be interpreted as a reduced packing density for the linactant molecules.

The spectral region used to characterize the fluorocarbon chains is presented in Figure 3b, which shows both the stretching and the bending modes of the CF_2 groups. In particular, the absorption bands at 1373 cm^{-1} and 1336 cm^{-1}, which are referred to as "axial CF_2" symmetric stretching bands with a strong component of the dynamic dipole moment along the helical axis,[42,55] are readily discernible for the fluorinated films derived from both **2** and **3**. These characteristic modes are commonly observed in thin organic films containing extended perfluorinated segments[45,55,56] and in the crystalline state for the pelletized partially

(51) Laibinis, P. E.; Whitesides, G. M.; Allara, D. L.; Tao, Y.-T.; Parikh, A. N.; Nuzzo, R. G. *J. Am. Chem. Soc.* **1991**, *113*, 7152.
(52) Snyder, R. G.; Strauss, H. L.; Elliger, C. A. *J. Phys. Chem.* **1982**, *86*, 5145.
(53) Bensebaa, F.; Ellis, T. H.; Badia, A.; Lennox, R. B. *Langmuir* **1998**, *14*, 2361.
(54) Bensebaa, F.; Ellis, T. H.; Badia, A.; Lennox, R. B. *J. Vac. Sci. Technol. A* **1995**, *13*, 1331.
(55) Lenk, T. J.; Hallmark, V. M.; Hoffmann, C. L.; Rabolt, J. F.; Castner, D. G.; Erdelen, C.; Ringsdorf, H. *Langmuir* **1994**, *10*, 4610.
(56) Tsao, M. W.; Hoffmann, C. L.; Rabolt, J. F.; Johnson, H. E.; Castner, D. G.; Erdelen, C.; Ringsdorf, H. *Langmuir* **1997**, *13*, 4317.

fluorinated thiols.[56,57] The observation of these axial bands is taken to indicate that the fluorocarbon parts of these molecules in the densely packed layers on the gold substrate retain the helical conformation of the respective bulk materials.[55]

The absorption bands in the 1150−1250 cm^{-1} region are also characteristic of perfluorinated alkyl chains.[55,58] An analysis of the infrared spectra of **3** in a prior study provides guidance for the interpretation of the IR peaks for **2** in this region.[56] The intense bands for **3** at ∼1151 cm^{-1}, ∼1205 cm^{-1}, and ∼1247 cm^{-1} arise predominantly from the symmetric and antisymmetric CF_2 stretching vibrations, where the dynamic dipole moment is perpendicular to the helical axis. In the double-chained thiol **2**, these motions might be dampened when they fall in the plane containing the second alkyl chain. Such dampening is complicated by the fact that **2** exists here as a pair of enantiomers, with the chiral center located at the branch point for the chain. This phenomenon might rationalize the diminishment of the two peaks at ∼1151 cm^{-1} and ∼1205 cm^{-1}, while the remaining peak at ∼1247 cm^{-1} appears to retain its intensity. If one compares the relative intensity of the axial and CF_2 stretching absorption bands in Figure 3b (parallel and perpendicular to the helical axis) and note that they are proportional to the average tilt angle of the fluorocarbon chains but are inversely affected by the tilt due to the surface selection rules for this IRRAS, it becomes apparent that the axial bands are proportionately smaller than the lone band associated with motion perpendicular to the chain at ∼1247 cm^{-1}. Since this relative intensity in the axial bands for the film of **2** is lower than that of **3**, we believe that the fluorocarbon chains in the SAMs derived from **2** are titled more from the surface normal than are those derived from **3**. Importantly, this interpretation is consistent with the XPS data (vide supra), which indicate a lower fluorocarbon density for the SAMs derived from **2** compared to those derived from **3**.

In the spectrum of the SAM derived from **1** (Figure 3b), none of the characteristic vibrations of fluorocarbon chains can be found. However, the methyl symmetric bending vibration appears at ∼1380 cm^{-1},[59] which is relatively insensitive to the conformational order of the remainder of the alkyl chain. In addition, the twisting-rocking (T_x) and wagging progression bands (W_x) are observed in the 1180−1380 cm^{-1} region.[59–61] The presence of these progression bands as a series of clearly defined peaks strongly indicates the crystalline nature of this SAM.

Conclusions

The targeted double-chained partially fluorinated linactant **2** was successfully prepared. The structure and conformation of the corresponding SAM on gold were characterized using a variety of techniques, and the results were compared to those obtained from SAMs derived from **1** and **3**. All three adsorbates bind to the gold substrate via their sulfur headgroups as in most related alkanethiolate-based SAMs on gold. The potential linactant **2** was found to form moderately ordered, loosely packed SAMs on gold, where the fluorocarbon moieties retain the expected helical conformation of the respective bulk material. Notably, the fluorocarbon density of the SAMs derived from **2** was less than that of the SAMs derived from **3**; correspondingly, the fluorocarbon helices in the SAM derived from **2** were more tilted from the surface normal than those derived from **3**. Additional experiments involving binary and ternary mixed monolayers are needed to develop an understanding of the effectiveness of linactant **2** in manipulating phase behavior.

Acknowledgment. We acknowledge generous financial support from the National Science Foundation (DMR-0447585 and DMR-0447588).

Supporting Information Available: Experimental details regarding the materials, procedures, and instrumentation used to conduct the research reported here. This information is available free of charge via the Internet at http://pubs.acs.org.

LA801397T

(57) Masetti, G.; Cabassi, F.; Morelli, G.; Zerbi, G. *Macromolecules* **1973**, *6*, 700.
(58) Chidsey, C. E. D.; Loiacono, D. N. *Langmuir* **1990**, *6*, 682.
(59) Hostetler, M. J.; Stokes, J. J.; Murray, R. W. *Langmuir* **1996**, *12*, 3604.
(60) Smith, E. L.; Porter, M. D. *J. Phys. Chem.* **1993**, *97*, 8032.
(61) Maroncelli, M.; Qi, S. P.; Strauss, H. L.; Snyder, R. G. *J. Am. Chem. Soc.* **1982**, *104*, 6237.